JOURNAL OF APPLIED POLYMER SCIENCE VOL. 16, PP. 2397-2415 (1972)

Surface Crosslinking of Polyethylene Using a Hydrogen Glow Discharge

MARTIN HUDIS, *Corporate Research and Development Center, General Electric Company, Schenectady, New York 12301*

Synopsis

Linear high-density polyethylene is crosslinked by exposing it to a hydrogen glow discharge and alternatively by exposing it to a low-pressure Hg–A ultraviolet lamp in a dry nitrogen atmosphere. For the UV lamp case, the crosslinked gel is measured as a function of the radiation dose. For the plasma case, the crosslinked gel is measured as a function of the exposure time. The two gelation curves are alternatively compared to an exponentially attenuated light theory and a diffusion theory. Excellent agreement exists between the measured gel-versus-dose curve and the theoretical curve based on the light theory for a monochromatic light beam at 1849 Å. The gelation curve for the hydrogen glow discharge case can be explained using the identical theory but applied to a spectrum of light covering the range from 1200 Å to 1900 Å. The different curves can be explained in terms of the different spectra. Energy transfer between the plasma and the polymer due to excited atoms, and/or charged particles, is not required to account for the different gel curves.

INTRODUCTION

Plasma polymer interactions are actively being studied because of their unique ability to surface modify polymers without affecting their bulk properties. Crosslinking is an example of a plasma polymer reaction and is produced when polyethylene is exposed to a hydrogen plasma. Previous work has demonstrated that ultraviolet radiation is an important if not the dominant mechanism through which a hydrogen plasma crosslinks polyethylene.[1] In spite of the fact that plasma crosslinking can be reduced to photochemistry for the hydrogen plasma case, drastic differences still exist between the gelation curves which result from exposure to a ultraviolet lamp compared with exposure to a hydrogen glow discharge. Plasma crosslinking produces a square root relationship between depth of penetration and radiation intensity,[2] while crosslinking with an ultraviolet lamp produces a logarithmic dependence on radiation intensity. The square root relationship has led people to suggest that plasma crosslinking unlike photochemical crosslinking may be produced by a diffusion process where hydrogen atoms or excitons are diffusing into the polymer.[2-4]

The object of this work is to compare various theories to experimental plasma crosslinking results. An exponential attenuated light theory and a

diffusion theory will be used as the two models. Assuming the diffusion theory is accurate, the diffusing species and its diffusion coefficient are important parameters which should be revealed by the study. If the attenuated light theory is accurate, the effective spectral components and the maximum depth of penetration are the important parameters which should be revealed by the study. In either case, these parameters are important in determining the overall usefulness of the process and the optimum system to be used.

The results of this experiment demonstrate that plasma crosslinking can be described using an exponentially attenuated light theory applied to a polychromatic ultraviolet spectrum. The polychromatic spectrum is required to produce the square root relationship between depth of penetration and radiation dose. In addition the experiment demonstrates that plasma crosslinking is limited to 10^{-2} cm and can be produced with the 1849 Å radiation from a low-pressure mercury ultraviolet lamp.

THEORY

Diffusion Model

The diffusion model is based on a solution to the diffusion equation for a semi-infinite polymer sample exposed to a monochromatic UV photon flux. A diffusion coefficient is assumed to exist independent of space and time which characterizes the crosslinking penetration. The crosslinking penetration is small compared to the thickness of the polymer sample in which case the polymer sample is assumed to be semi-infinite. The active species (mass or energy) are assumed to be generated in a thin layer compared to the depth of penetration. The crosslinking concentration at the plasma polymer interface is assumed to be constant and is the boundary condition for the diffusion problem. For these conditions, the solution to the diffusion equation is trivial and is shown in eq. (1):

$$\delta_x = \delta_0 \int_{x/\sqrt{Dt}}^{\infty} d\eta \, e^{-\eta^2} \tag{1}$$

where δ_x is the number of crosslinks at position x per primary weight average molecular weight and δ_0 is the boundary value at the polymer plasma interface. For these experiments, the gel mass (M_G) is the specific quantity of interest. If g_x is the gel content at position x per unit volume, then the gel mass is attained through Eq. (2):

$$M_G = \rho A \int_0^{x^*} dx g_x \tag{2}$$

where ρ(g cm^{-3}) is the polymer density, A (cm^2) is the irradiation area and x^* is the incipient gel point within the polymer. For a given polymer distribution, one can relate g_x to δ_x and evaluate the integral analytically or

at least numerically. Although the procedure is straightforward, the physics is more transparent if an approximate solution is obtained as outlined below.

For $\delta_x \gtrsim 10$, $g_x \cong 1$ which simplifies eq. (2) to eq. (3):

$$M_G = \rho A \left\{ \int_0^{x(\delta=10)} dx + \int_{10}^{1} g_x \frac{dx}{d\delta_x} d\delta_x \right\}. \tag{3}$$

The diffusion model characterized by eq. (3) has two important properties which can be compared to experimental data. Equation (3) predicts that gelation mass is a linear function on a square root-of-time scale. This property is a direct consequence of the constant boundary condition. For the case of an aribtrary boundary condition, the solution to the diffusion equation is well defined, and an analogous calculation demonstrates that the gelation mass is *not* a linear function on a square root-of-time scale. The second property is related to the slope of the gelation curve when plotted on a square root-of-time scale. The incipient gel point is an increasing function of the initial weight-average molecular weight ($\bar{M}_{w0}$) of the polymer in which case from eqs. (1) and (3) one sees that the slope of the gelation curve when plotted on a square root-of-time scale is proportional to the initial weight-average molecular weight.

Attenuated Light Model

Analytical treatments of random linear polymer chain crosslinking caused by exponentially attenuated radiation (UV light) have been available for many years. If one assumes the absorbed UV energy obeys Beer's law, then the energy absorbed at position x (cm) per gram of polymer and per unit wavelength is given by eq. (4):

$$R_x(\lambda) = t\bar{v}I(\lambda)\, k(\lambda)\, e^{-kx} \tag{4}$$

where t (sec) is the exposure time, $\bar{v}$ (cm^3/g) is the specific volume of the polymer, $I(\lambda)$ (photons/cm^2-sec) is the radiation intensity, and k (cm^{-1}) is the absorption coefficient at wavelength λ (Å). In general, the absorption coefficient will change with time, but for simplicity it is assumed constant. If one neglects scissioning and only considers crosslinking, then the number of crosslinks at position x per primary weight-average molecular weight and per unit wavelength is given by eq. (5):

$$\delta_x(\lambda) = (\bar{M}_{w0}\phi(\lambda)/N)R_x(\lambda) \tag{5}$$

where $\phi(\lambda)$ is the number of crosslinks per absorbed photon and N is Avogadro's number. The gel mass is again the specific quantity of interest and is obtained from eq. (6):

$$M_G = \rho A \int_0^{\infty} d\lambda \int_0^{x^*} dx g_x(\lambda). \tag{6}$$

Following the work of Shultz,[5] the analytical relationship between $g_x(\lambda)$ and $\delta_x(\lambda)$ shown in eq. (7) for the polymer distribution shown in eq. (8) is used to evaluate the integrals in eq. (6):

$$1 - g_x(\lambda) = \left\{1 + \frac{\delta_x(\lambda)g_x(\lambda)}{Z+1}\right\}^{-(Z+1)} \tag{7}$$

$$W(M_N) = \frac{M_N{}^Z \eta^{Z+1} e^{-\eta M_N}}{\Gamma(Z+1)} \tag{8}$$

where $\eta = Z/\bar{M}_N = (Z+1)/\bar{M}_w$ and Z is an arbitrary positive number.

Shultz[6] has evaluated the integral when the light beam is monochromatic and the polymer has a most probable distribution ($Z = 1$). The results are shown in eq. (9):

$$\frac{M_G k}{\rho A} = f(R_0/R^*) \tag{9}$$

where $R_0 = tvkI$ and $R^* = N/\bar{M}_w\phi$. When the light beam is not monochromatic and/or the polymer is not represented by a most probable distribution, eq. (6) is more difficult to evaluate but can be evaluated numerically.

EXPERIMENTAL

The glow discharge apparatus and the procedure for obtaining the gelation mass have been described before.[1]

Figure 1 is a graph of gelation mass on a square root-of-time scale for polymer samples with different initial weight-average molecular weights. The plasma conditions have been kept constant during the whole experiment. Note that the curves are linear, and for the two Marlex samples the slope of the curve is proportional to the weight-average molecular weight. The lack of agreement between irradiated similar samples produced by different manufacturers can be traced to the impurities within the material. These data are very similar to results published by Schonhorn[2] and is consistent with one of the fundamental properties of eq. (3).

The second fundamental property of eq. (3) was investigated by measuring the crosslinking concentration at the surface of the plasma irradiated sample. These measurements were made using the apparatus shown in Figure 2. The crosslinked layer is supported in a heated solution of paraxylene, and a cathetometer is used to measure the linear swelling. The cathetometer is focused on the bottom of the crosslinked layer. Measurements were first made on high-energy electron irradiated polyethylene samples to verify that the measurements represent swelling and not elastic stretching. These measurements are shown in Figure 3. The swelling measurements on high-energy electron-irradiated polyethylene agrees with those contained in the literature[7] and Flory's theory,[8] which predicts swelling is proportional to dose rate. Swelling measurements for

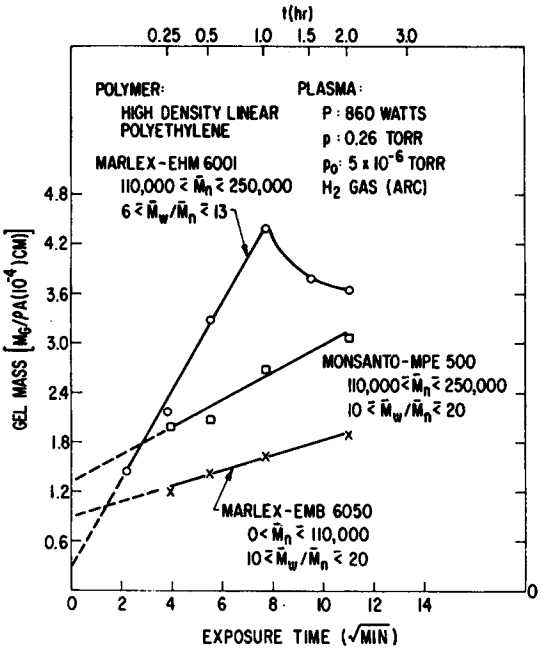

Fig. 1. Plasma crosslinking gel curves for three different polymers each having different molecular weights.

plasma-crosslinked polyethylene as a function of temperature and time are shown in Figure 4. Note that the crosslinking concentration at the boundary of the polymer sample is not constant but increases with exposure time. This observation is inconsistent with eq. (3).

A curve of gel mass versus radiation dose derived from eq. (9) is plotted in Figure 5. The dashed line has a slope of $^1/_2$ and represents a square root-of-time dependence. The gelation data from my previous work (see ref. 1) is also plotted in Figure 5 using k, I, and ϕ as free parameters. The dots are the data from the integrated system, while the crosses are the data from the separated system. Although there is reasonable agreement over a limited radiation range, if the range is extended in either direction, definite deviations appear. If one nelgects this lack of agreement for the moment and assumes crosslinking is caused by a monochromatic light beam, the effective wavelength can be predicted from the curve in Figure 5, the data in ref. 1, and the polyethylene UV absorption spectrum.[9] The effective wavelength predicted from the data is 1850 Å, which is *not* strongly absorbed by polyethylene as had been assumed in earlier plasma work. This is an important observation because radiation at 1850 Å is not absorbed in a thin surface layer compared with the crosslinking depth of penetration, in which case a diffusion model becomes harder to justify.

The advent of low-pressure mercury UV lamps allows one to easily verify this observation. Low-pressure mercury lamps using Spectrosil quartz

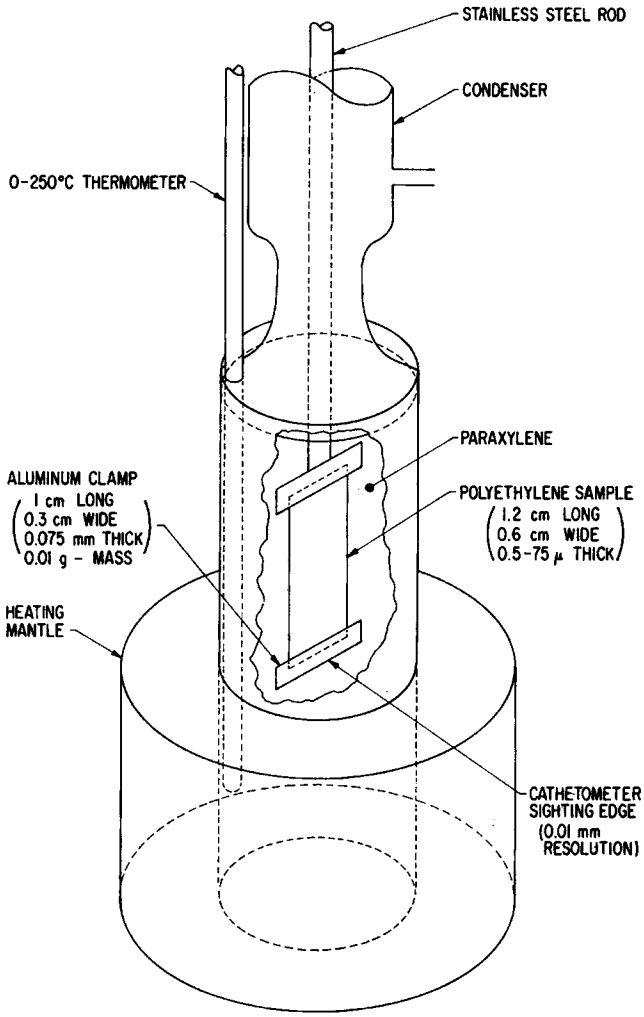

Fig. 2. Apparatus used to measure swelling in thin crosslinked polymer samples.

envelopes have a large flux density at 1849 Å. A large flux density also exists at 1942 Å and 2537 Å, but pure high-density polyethylene is transparent at these wavelengths. The identical polyethylene used in the plasma experiments was irradiated in a dry nitrogen atmosphere using a low-pressure mercury argon UV lamp (supplied by P. D. Johnson). The system consists of two concentric cylinders. The inner cylinder is 1 in. in diameter and is the UV lamp. The outer cylinder is 2 in. in diameter and contains the flowing dry nitrogen (2 ft^3/hr) and the polyethylene sample (attached directly to the UV lamp). The gelation data are plotted as a dashed line in Figure 6. The solid curve is the identical theoretical curve shown in Figure 5. The intensity of the 1849 Å line has been calibrated by

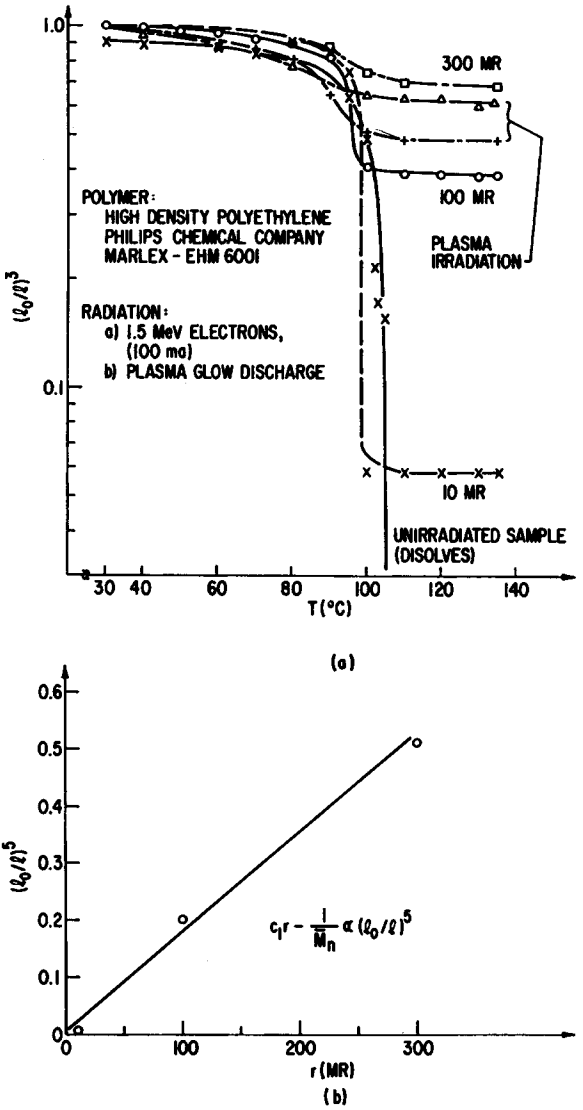

Fig. 3. Swelling data as a function of the solvent temperature: (a) comparison between unirradiated samples, high-energy electron irradiated samples, and plasma-irradiated samples; (b) swelling ratio for high-energy electron irradiated samples as a function of dose rate.

P. D. Johnson in watts per cm^2 as a function of current density.[10] The quantum yield is, therefore, the only free parameter and is uniquely defined by the two curves in Figure 6. The UV lamp is run at 0.8 amp (0.3 amp/cm^2) producing a flux of 0.017 watt/cm^2. For Marlex EHB-6002, $\bar{v} = 1.04$ and $\bar{M}_{N0} \cong 1.2 \times 10^4$, in which case $\phi = 5 \times 10^{-4}$ xl/absorbed photon.

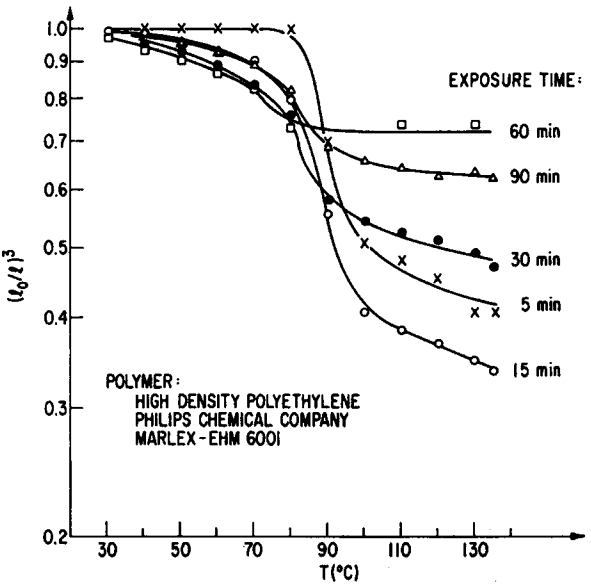

Fig. 4. Swelling data as a function of solvent temperature and exposure time for plasma-irradiated samples.

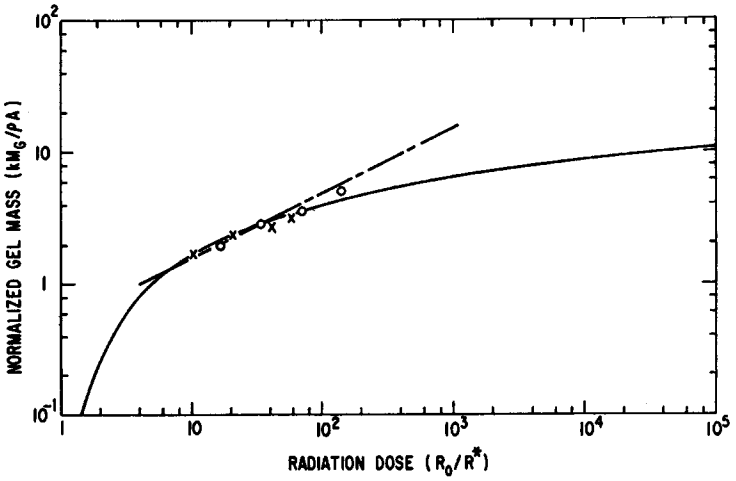

Fig. 5. Solid curve is a plot of eq. (9); (×) and (○) are experimental data taken from ref. 1.

Plasma and UV lamp crosslinking data over an extended time scale are plotted in Figure 7. The hydrogen plasma and the UV lamp produce different crosslinking dose curves. The plasma data is obtained using the integrated system discussed in ref. 1. The dashed line is again proportional to the square root of time. The UV lamp data agrees with the theory for a monochromatic light beam, while the plasma case has a square root-of-time dependence and does not agree with the theory.

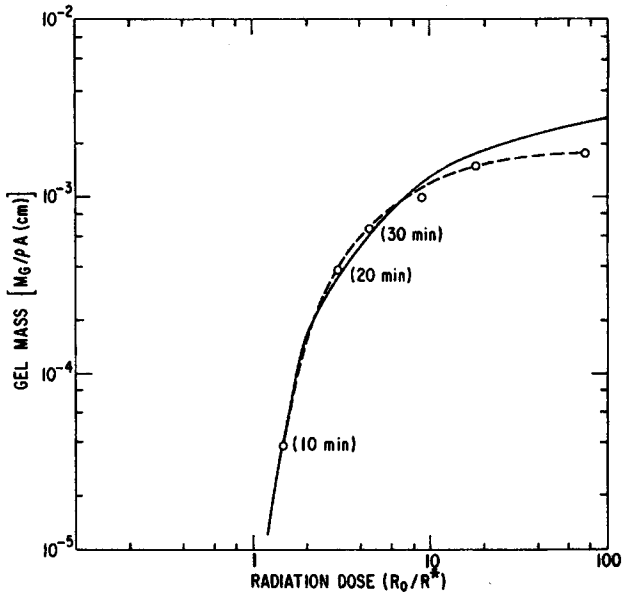

Fig. 6. Gelation mass vs. radiation dose. Solid line is plot of eq. (9); dashed line is data for irradiation with UV lamp.

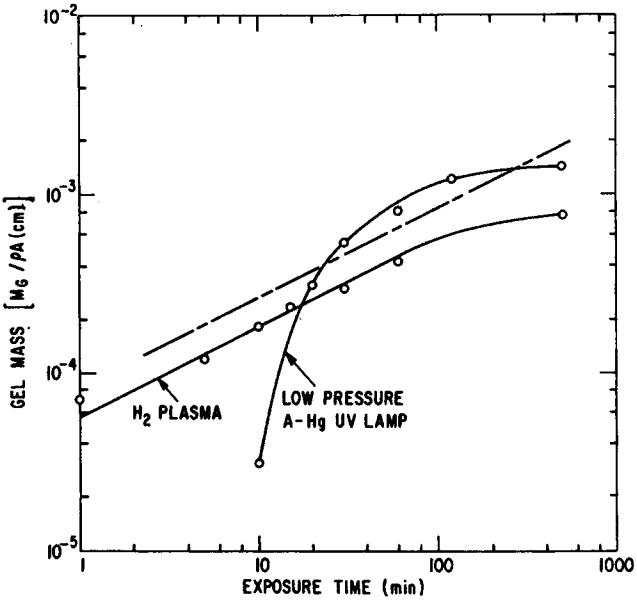

Fig. 7. Measurements of gelation mass vs. exposure time for exposure with hydrogen plasma and exposure with UV lamp.

The theoretical curves in Figures 5 and 6 have been derived for a most probable polymer distribution ($\bar{M}_w/\bar{M}_N = 2$). For Marlex EHB-6002, $10 < \bar{M}_w/\bar{M}_N < 20$, in which case the polymer distribution is broader than a most probable distribution. A broader distribution should stretch the theoretical curve in Figure 5 and may yield a curve with a square root dependence. This possibility was investigated by comparing the gelation curves for $Z = 1$ and for $Z = 0.07$ ($\bar{M}_w/\bar{M}_N = 15$), as shown in Figure 8.

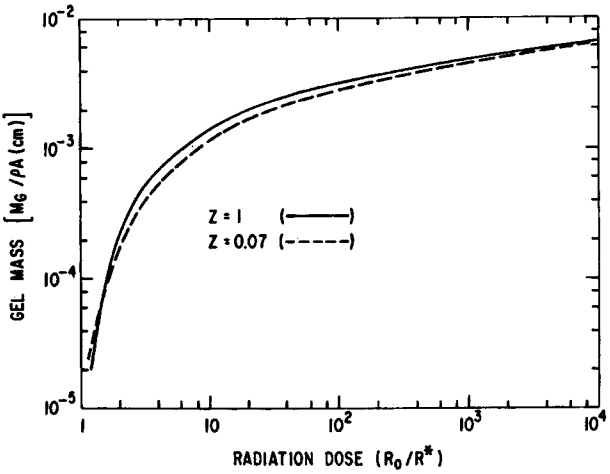

Fig. 8. Plot of eq. (9). Solid curve is for a most probable distribution, dashed curve is for a broader distribution.

The $Z = 0.07$ curve is obtained by numerical integration. Little difference exists between the two curves. One is not able to explain the square root dependence in terms of the polymer distribution. This is not surprising in light of the excellent agreement which exists between the theory for a most probable distribution and the experiment using a UV lamp. The reason for the insensitivity is apparent when one examines the distributions plotted in Figure 9. The smaller molecules ($M < 10^5$) in the broader distribution do not readily crosslink. Although these molecules do not gel, they represent a small fraction of the polymer mass and are experimentally unimportant. The larger molecules ($M > 10^5$) in the broader distribution begin to gel before the molecules in a most probable distribution of the same number-average molecular weight. This effect can be seen in the crossover of the two curves in Figure 8, at $R_0/R^* \cong 1.4$. Again, the overall effect appears to be very slight. The different properties produced by the plasma and the UV lamp must have their origin in the different spectra.

The effect of a polychromatic beam was investigated by considering a two component light beam. For this case, eq. (5) is transformed to eq. (10):

$$\delta_x(\lambda) = (\bar{M}_{w0}\, t\bar{v}/N) \sum_{i=1}^{2} k_i \phi_i I_i\, e^{-kix} \qquad (10)$$

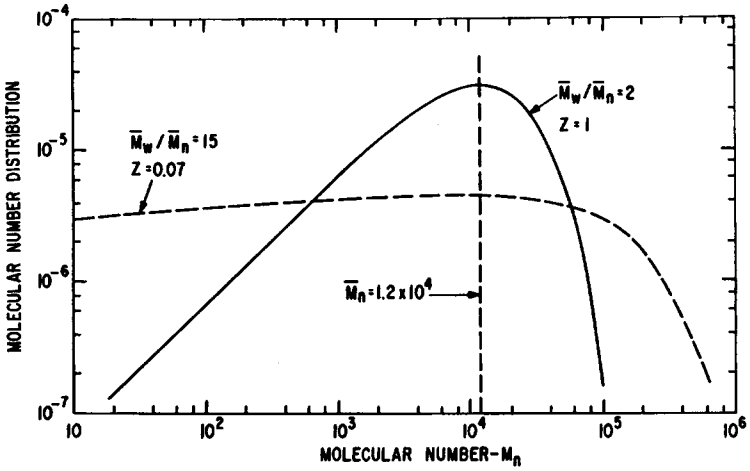

Fig. 9. Molecular number distribution curves used in deriving curves in Figure 8.

For this example, I_t is a free parameter in which case ϕ_1 can be set equal to ϕ_2, producing eq. (11):

$$\delta_x(\lambda) = (R_0(\lambda_1)/R^*(\lambda_1))\left\{e^{-k_1 x} + \frac{\lambda_2 I_2}{\lambda_1 I_1} e^{-k_2 x}\right\}. \tag{11}$$

If eqs. (11) and (7) are cross-plotted to give $g_x(\lambda_2 I_2/\lambda_1 I_1)$ as a function of x, then eq. (6) can be numerically integrated. Results for $k_1 = 1.27\times10^3$ and $k_2 = 1\times10^4$ cm^{-1} are shown in Figure 10. The shape of the gel curve is drastically altered by the second spectral component. Through proper choice of the spectrum, a large linear region with a slope of $^1/_2$ can be obtained.

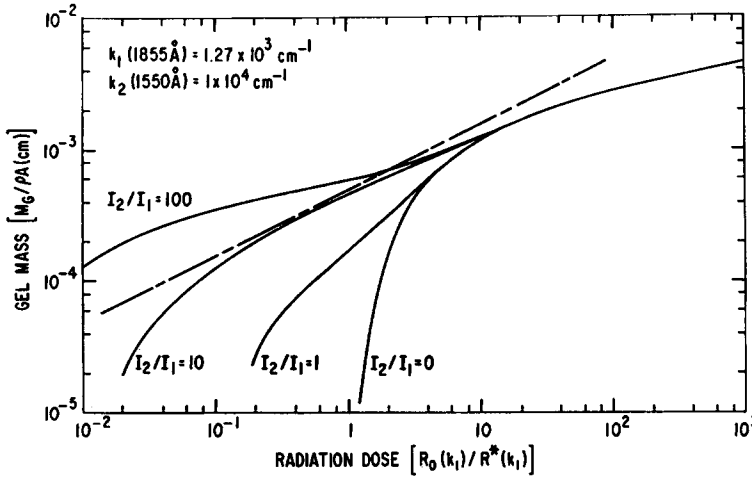

Fig. 10. Gelation mass vs. radiation dose derived from eqs. (7), (11), and (6).

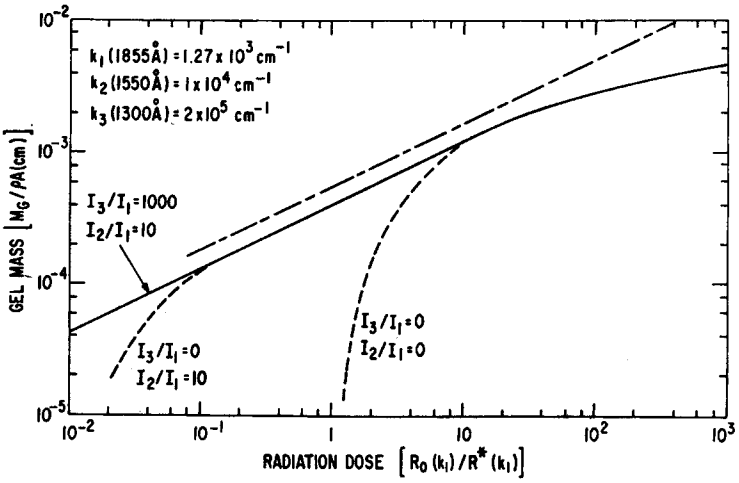

Fig. 11. Gelation mass. vs. radiation dose for three-component UV light beam. The ratio of the light intensities are chosen to give a linear curve with a slope of $^1/_2$.

The polyethylene UV absorption spectrum for $\lambda \gtrsim 1200$ Å can be approximated by three rectangular regions. One region is the absorption around 1850 Å due to the ethylene structure ($k = 1.27 \times 10^3$ cm^{-1}), the second is a nonionizing absorption ($k = 20 \times 10^5$ cm^{-1}), and the third is the transition region ($k = 1 \times 10^4$ cm^{-1}). The gel curve for these three components is shown in Figure 11. The intensity ratios have been chosen to yield a linear gel curve with a slope of $^1/_2$. A gel curve with a square root dependence over an extended dose scale can be obtained from a polychromatic spectrum. There is no need to invoke direct energy transfer from the plasma to the polymer and/or a diffusion model, as has been suggested in previous plasma work.

The plasma gelation curve plotted on a square root-of-time scale is linear and has a slope which is a function of the UV flux. According to the theory presented in the theory section, the slope is proportional to the square root of the UV flux. An experiment was performed in which the UV flux and spectrum from a hydrogen plasma were measured and compared to the slope of the gelation curve. The results from the experiment supply additional evidence which demonstrate that the UV flux is the dominant coupling which occurs between the plasma and the polymer. Figure 12 shows the apparatus used to measure the plasma spectrum and relative changes in the flux.[11] The UV detector is installed in the apparatus discussed in ref. 1. In contrast to the earlier work, a lithium fluoride window now isolates the polymer from the plasma. Four optical filters are used to divide the spectrum into four regions. Figure 13 shows typical data for five separate plasma cases. Gelation data for polyethylene irradiated in a low-pressure argon atmosphere by a hydrogen plasma through a lithium fluoride window is shown in Figure 14. The ratio of the slopes for the two gel curves shown

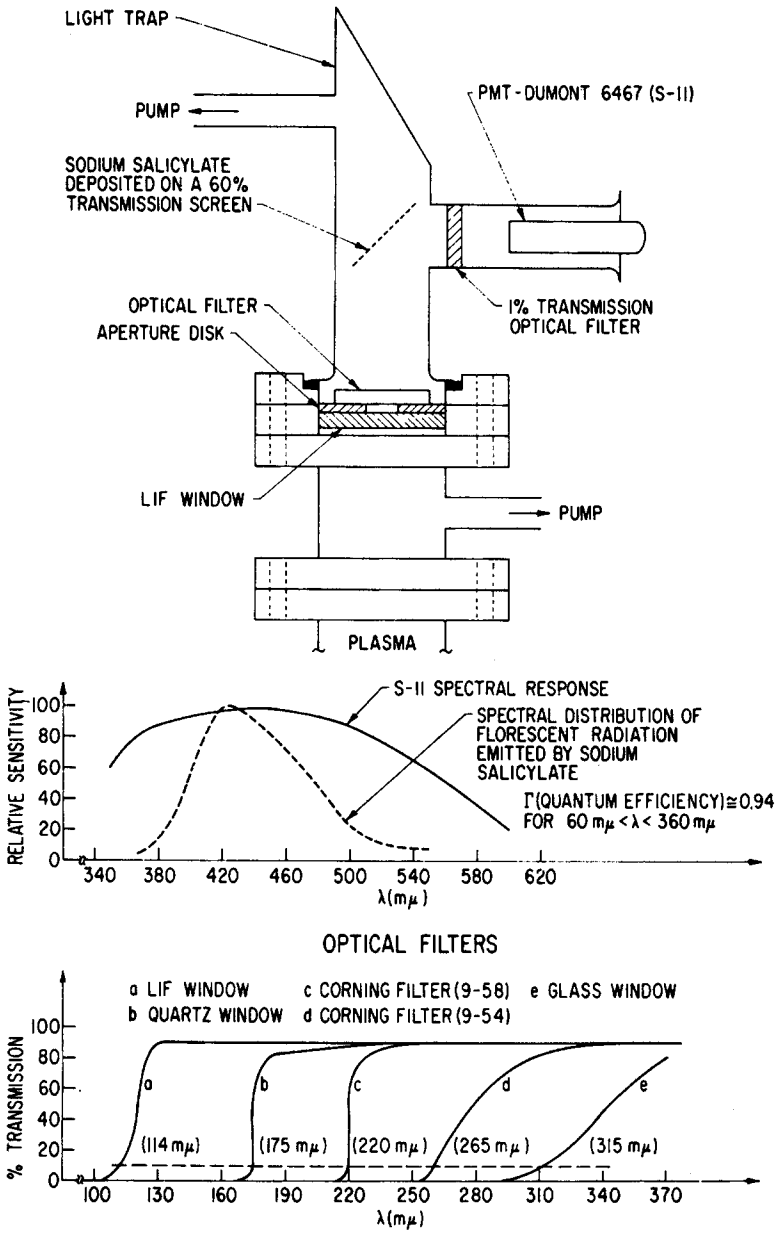

Fig. 12. Apparatus used to measure relative changes in the UV spectrum corresponding to changes in the hydrogen discharge.

in Figure 14 corresponding to the clean hydrogen case ($p_0 = 5 \times 10^{-6}$ torr) is equal to 0.5. The square root of the ratio of the light intensities equals 0.55. Note that the spectra remain invariant in going from the glow mode to the arc mode. The excellent agreement is surprising.

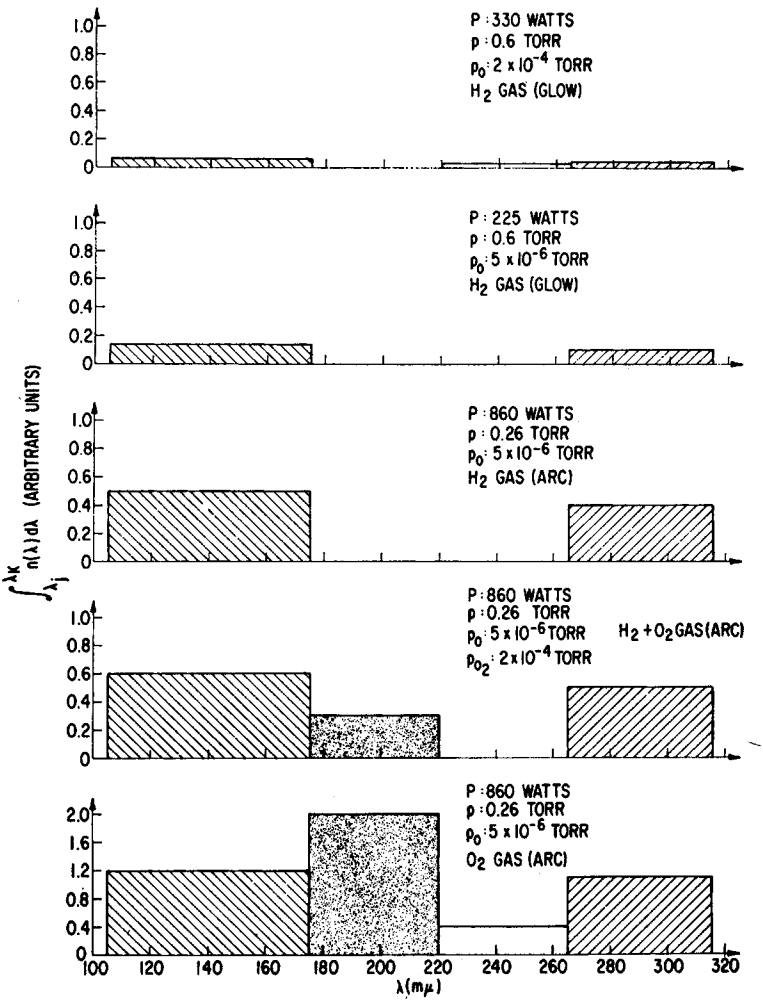

Fig. 13. Ultraviolet spectrum produced by hydrogen glow discharge; p_0 is system base pressure and p is operating pressure.

One can drastically alter the spectrum by adding impurities to the gas, such as using a higher base pressure or by adding oxygen. The change in the spectrum (Fig. 13) has a drastic effect on the gelation curve, as indicated by the data in Figure 14. These effects were not studied.

Spectrophotometry data in Figure 15 is additional evidence which is consistent with the attenuated light theory for a photon flux at 1850 Å. Attenuated total reflectance measurements before and after plasma irradiation are shown in Figure 15b. Transmission measurements before and after plasma irradiation are shown in Figure 15a. The transmission spectrum was obtained from six combined crosslinked layers each removed intact from the irradiated polymer sample. Note that the attenuated total

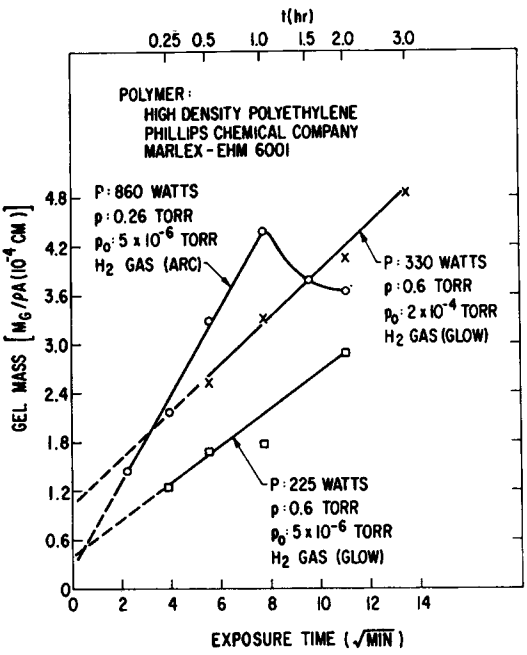

Fig. 14. Gelation mass curves produced by exposure to three different hydrogen plasmas.

reflectance data indicates an increase in the concentration of *trans*-vinylene bonds and a decrease in the concentration of vinyl bonds. This is only qualitative information but is consistent with previous measurements made by Schonhorn and Hansen.[2] The transmission data reveal quantitative information and demonstrate that the vinyl concentration in the crosslinked layer is negligible while the *trans*-vinylene concentration $\cong 8\times10^{-2}$ moles/l. ($\epsilon \equiv$ molar extinction coefficient = 139 l./mol-cm).

The final piece of data is contained in Figure 16 and is a gelation graph for a plasma-irradiated sample at two different polymer temperatures. Note that the slope of the curve decreases when the polymer temperature is increased from 25°C to 85°C. These temperature data are inconsistent with the diffusion model characterized by eq. (3). According to eq. (3), the gelation slope is proportional to the diffusion coefficient, which should be an increasing function of temperature.

DISCUSSION

The crosslinking concentration data (Fig. 4), the gelation temperature data (Fig. 16), and the effective spectral component data (Fig. 5) demonstrate that a diffusion model does not explain plasma crosslinking. The dominant properties of plasma crosslinking can be explained using a polychromatic exponential attenuated light theory. One does not have to in-

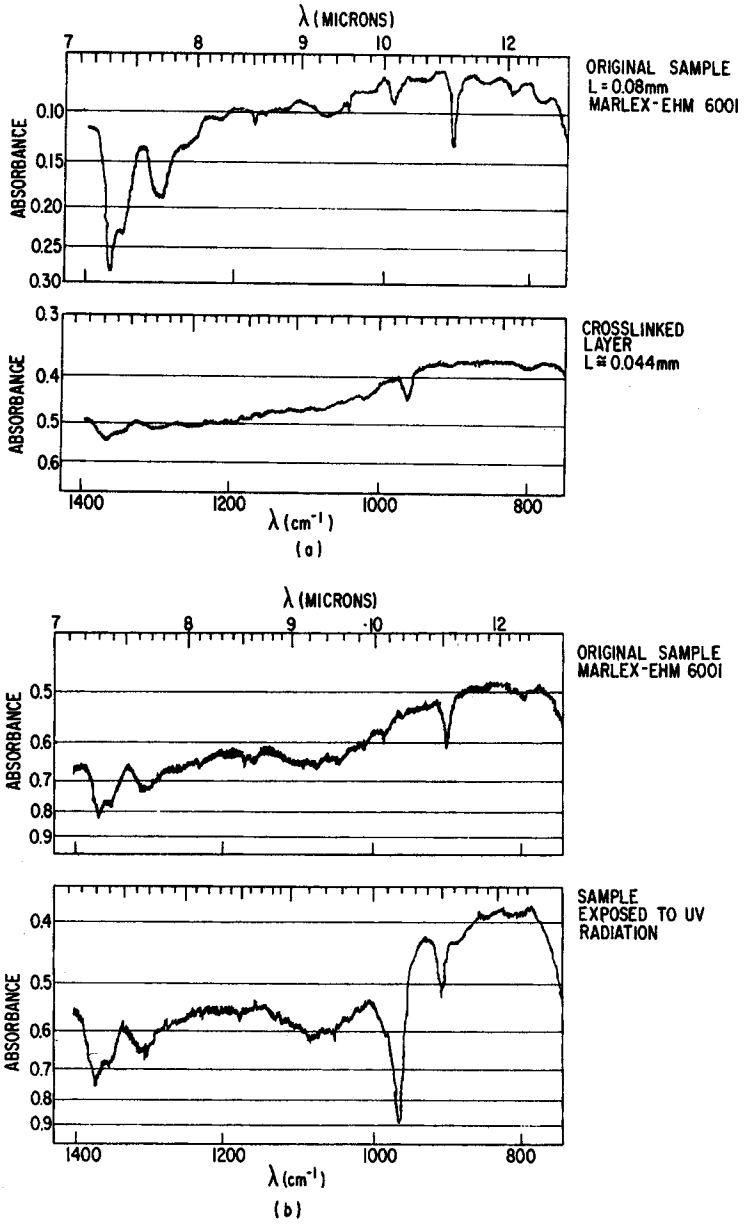

Fig. 15. Spectrophotometry data: (a) infrared transmission spectrum of original sample and removed crosslinked layer; (b) infrared ATR spectrum of original sample and plasma-irradiated sample.

voke direct energy transfer mechanism between the plasma and the polymer to explain the results.

The measured quantum yield (5×10^{-4} xl/photon at 1849 Å) is small when compared to G values for high-energy radiation crosslinking. G

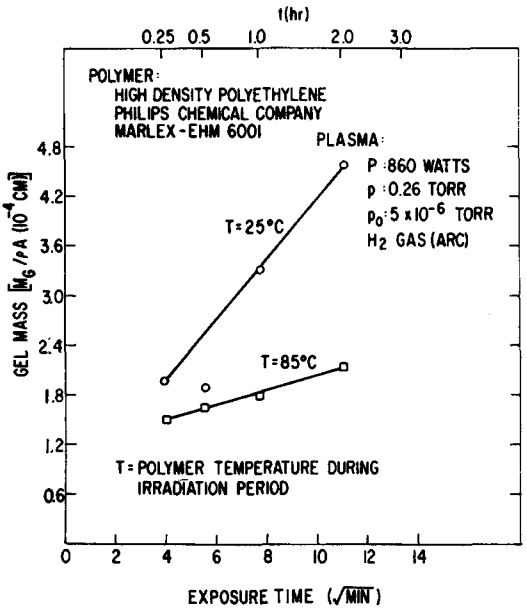

Fig. 16. Gelation curves for a polymer exposed to plasma at different polymer temperatures.

values for polyethylene crosslinking are typically 1–4 xl/100 eV of absorbed energy. The high-energy radiation process is 100–500 times more effective than the UV radiation. Although the difference in yield is enormous, it is not inconsistent with other comparisons in the literature.[12] Charlesby and Partridge[13] compare the yield for alkyl production in polyethylene using a UV lamp (Hanovia, 2537 Å) in one case and γ-radiation for the second case. They found the γ-radiation to be 120 times more effective than the UV radiation.

The swelling data in Figure 3a demonstrates that plasma irradiation (UV irradiation) can produce a relatively large crosslinking concentration. The crosslinking concentration can be crudely estimated from the swelling data and Flory's[8] equation, which relates swelling to crosslinking. The theory is based on the assumptions that crosslinks are randomly located and have a spatially uniform concentration. These assumptions are not valid for plasma crosslinking. Nevertheless, if the theory is blindly applied, a crude estimate is obtained which predicts the average molecular weight between crosslinks to lie in the range between 220 and 610 amu.

CONCLUSIONS

An experiment has been performed which compares two distinct processes for crosslinking polyethylene. The first process irradiates polyethylene with a low-pressure mercury–argon UV lamp. The second process irradiates polyethylene with a hydrogen glow discharge. The results of the

experiment demonstrate that hydrogen plasma crosslinking can be completely accounted for using an established UV light irradiation theory applied to a UV light beam containing spectral components in the range 1200–1900 Å. One does not have to invoke direct energy transfer mechanisms between the plasma and the polymer (such as bombardment by metastables) or a diffusion process within the polymer to explain the differences between the two experiments. The plasma acts as a broad-band UV lamp.

The quantum yield for crosslinking high-density polyethylene with 1849 Å UV photons was measured and is equal to 5×10^{-4} xl/photon. Crosslinking of high-density linear polyethylene with UV radiation is extremely inefficient compared to high-energy radiation processes.

The exponentially attenuated UV light theory predicts that the depth of penetration depends logarithmically on radiation dose, for doses in excess of 10 times the gelation dose. Plasma polymer treatments that are dominated by UV coupling are, therefore, primarily surface treatments with penetrations limited to 10^{-3} to 10^{-2} cm.

List of Symbols

g_x	gel content per unit volume at position x
$k(\lambda)$	absorption coefficient at wavelength λ
p	discharge gas pressure
p_0	chamber base pressure
t	irradiation exposure time
$\bar{v}$	polymer specific volume
x	distance within the polymer sample
x^*	incident gel position
A	irradiation area
D	diffusion coefficient
G	number of crosslinks per 100 eV of absorbed energy
$I(\lambda)$	radiation intensity
M_G	gel mass
M_N	molecular number
$\bar{M}_N$	number-average molecular weight
$\bar{M}_{N0}$	initial number-average molecular weight
$\bar{M}_w$	weight-average molecular weight
$\bar{M}_{w0}$	initial weight-average molecular weight
N	Avogadro's number
$R_0(\lambda)$	energy absorbed per gram of polymer about wavelength λ at the polymer surface
$R_x(\lambda)$	energy absorbed per gram of polymer about wavelength λ at position x
R^*	incipient gel radiation dose
$W(M_N)$	molecular number distribution
δ_0	number of crosslinks per primary weight-average molecular weight at the polymer surface

δ_x number of crosslinks per primary weight-average molecular weight at position x
ϵ molecular extinction coefficient
ρ polymer density
λ ultraviolet radiation wavelength
$\phi(\lambda)$ number of crosslinks per absorbed photon about wavelength λ

The author wishes to acknowledge the helpful discussions and theoretical information provided by Allan R. Shultz. The author also wishes to thank P. D. Johnson for the use of the UV mercury–argon lamp, R. S. McDonald for taking the spectrophotometry data, and L. E. Prescott for building and maintaining the equipment.

References

1. M. Hudis and L. E. Prescott, *J. Polym. Sci., B*, **10**, 179 (1972).
2. H. Schonhorn and R. H. Hansen, *J. Appl. Polym. Sci.*, **11**, 1461 (1967).
3. R. H. Hansen and H. Schonhorn, *J. Polym. Sci. B*, **4**, 203 (1966).
4. J. R. Hall, C. A. L. Westerdahl, A. T. Devine, and M. J. Bodnar, *J. Appl. Polym. Sci.*, **13**, 2085 (1969).
5. A. R. Shultz, Preprint 241, Nuclear Engr. and Sci. Congress Meeting, (Cleveland, Ohio, Dec. 1955), Amer. Inst. of Chem. Engr., New York.
6. A. R. Shultz, *J. Chem. Phys.*, **29**, 200 (1958).
7. A. Charlesby, *Atomic Radiation and Polymers*, Pergamon Press, New York, 1960, p. 214.
8. P. J. Flory, *Principles of Polymer Chemistry*, Cornell University Press, Ithaca, N. Y., 1953, p. 579.
9. R. H. Partridge, *J. Chem. Phys.*, **45**, 1695 (1966).
10. P. D. Johnson, *J. Opt. Soc. Amer.*, **61**, 1451 (1971).
11. R. Allison, J. Burns, and A. J. Tuzzolino, *J. Opt. Soc. Amer.*, **54**, 747 (1964).
12. B. Raney and H. Yoshida, *J. Polym. Sci. C*, **12**, 263 (1966).
13. A. Charlesby and R. H. Partridge, *Proc. Roy. Soc.*(London), **A283**, 329 (1965).

Received February 17, 1972